Available online at www.sciencedirect.com
ScienceDirect
Trans. Nonferrous Met. Soc. China 35(2025) 2762−2776
Transactions of Nonferrous Metals Society of China
www.tnmsc.cn

Efficient oxidation of thiosulfate in solution using multistage method

Hao-ran XU[1], Wei-chao HUANG[2], A. V. RAVINDRA[3], Duc-lenh PHAN[4], Thi-quynh-xuan LE[1], Li-bo ZHANG[1], Shao-hua YIN[1]

1. School of Metallurgical and Energy Engineering, Kunming University of Science and Technology, Kunming 650093, China;
2. China Rare Earth (Guangxi) Jinyuan Rare Earth New Materials Co., Ltd., Hezhou 542603, China;
3. Department of Physics and Nanotechnology, Faculty of Engineering and Technology, SRM Institute of Science and Technology, Kattankulathur, Tamil Nadu 603203, India;
4. Science and Technology Center, MienTrung Industry and Trade College, Phu Yen 56000, Viet Nam

Received 16 December 2023; accepted 3 July 2024

Abstract: The oxidation characteristics of sulfite and thiosulfate were examined by using thermodynamic calculations and simulated desulfurization solution experiments to investigate their difference. Subsequently, a new multistage oxidation method using oxygen−ammonium persulfate was presented and applied to the oxidation of a real desulfurization solution. The results show that the concentrations of thiosulfate and sulfite in the real desulfurization solution decrease from 48.76 and 61.76 g/L to 2.24 and 0.02 g/L, respectively, and the ammonium sulfate products obtained are white with uniform particles. In addition, compared with ammonium persulfate alone, the multistage oxidation method can reduce the ammonium persulfate addition by 37.56% and treatment cost by 28.13%.
Key words: ammonium persulfate; oxygen; thiosulfate; desulfurization solution; cost

1 Introduction

Flue gas desulfurization is a vital link in the discharge of non-ferrous smelters, which plays a significant role in reducing air pollution [1−3]. Among the existing flue gas desulfurization processes, ammonia desulfurization has been widely used in industrial flue gas treatment due to its high desulfurization efficiency, low energy consumption, low carbon dioxide emissions, and complete resource utilization of by-product ammonium sulfate [4−6]. The principle of ammonia desulfurization is to use ammonia to absorb sulfur dioxide in the flue gas to form a desulfurization solution mainly composed of ammonium sulfite, and then use an oxidant to oxidize ammonium sulfite into ammonium sulfate products that can be used as agricultural fertilizer.

However, thiosulfate ($S_2O_3^{2-}$), a sulfur-containing impurity, becomes easily enriched in the desulfurization solution when the ammonia desulfurization system is operated for a long time. Once the $S_2O_3^{2-}$ content in the desulfurization solution exceeds the standard level, it causes problems such as the generation of sulfur impurities during the oxidation step, a decrease in the sulfite oxidation efficiency, and deterioration of the chromaticity and quality of the ammonium sulfate product.

The primary approaches for removing $S_2O_3^{2-}$ from the desulfurization solution include membrane

Corresponding author: Thi-quynh-xuan LE: Tel: +86-15288498983, E-mail: quynhxuanlt@kust.edu.cn;
Li-bo ZHANG, Tel: +86-13888310177, E-mail: zhanglibopaper@126.com
https://doi.org/10.1016/S1003-6326(25)66846-4

filtration [7], anion exchange resin [8,9], and conversion into sulfur-combined separating methods [10,11]. Although membrane filtration has high separation efficiency, it has disadvantages such as high membrane price, easy blockage and pollution, and high operation and maintenance cost. The anion exchange method has problems, such as low thiosulfate removal rate and high resin consumption. To convert thiosulfate into sulfur, the principle is to add concentrated sulfuric acid or microorganisms and then separate the formed sulfur impurities. However, this method still has issues with a complex process, complicated operation, high cost, and incomplete separation of sulfur. In this case, a satisfactory treatment option is to involve converting ammonium thiosulfate in solution to ammonium sulfate product.

The most commonly utilized oxidants in the industry are concentrated sulfuric acid (H_2SO_4), hydrogen peroxide (H_2O_2), and oxygen (O_2). However, concentrated H_2SO_4 is not a suitable oxidant for treating desulfurization solutions containing $S_2O_3^{2-}$ because $S_2O_3^{2-}$ is extremely unstable under acidic conditions and rapidly decomposes to form sulfur. H_2O_2 was also found to convert $S_2O_3^{2-}$ into unstable polythionate intermediate products in addition to sulfate products, which further decomposed to form sulfur [12]. Oxygen is an inexpensive oxidizing agent used in industry because it does not produce other impurities when reacting with sulfite (SO_3^{2-}) and $S_2O_3^{2-}$, but the oxidation efficiency of $S_2O_3^{2-}$ by oxygen is notably low, reaching only approximately 20% [13,14].

In our recent work [15], we reported that ammonium persulfate ($(NH_4)_2S_2O_8$) is an ideal oxidant for oxidizing thiosulfate-containing desulfurization solutions and producing qualified ammonium sulfate fertilizer [16]. However, the use of ammonium persulfate oxidation alone requires a high dosage of ammonium persulfate oxidant, and the price of ammonium persulfate (500−600 US$/t) is much higher than that of concentrated H_2SO_4, O_2 and other oxidants used in ammonia desulfurization, limiting its industry application. Considering that $S_2O_3^{2-}$ and SO_3^{2-} coexist in the desulfurization solution, it is necessary to study the oxidation characteristics of $S_2O_3^{2-}$ and SO_3^{2-} under different oxidant conditions and to develop an efficient and economical oxidation treatment technology for high- concentration $S_2O_3^{2-}$ desulfurization solutions by combining several technologies to reduce the use of $(NH_4)_2S_2O_8$.

Based on the difference in the oxidation characteristics of $S_2O_3^{2-}$ and SO_3^{2-} under different oxidants (O_2, $(NH_4)_2S_2O_8$), a new oxygen−ammonium persulfate oxidation technology has been proposed to treat desulfurization solutions containing $S_2O_3^{2-}$. The idea is to use inexpensive O_2 to oxidize most of the SO_3^{2-} in the desulfurization solution to sulfate and then use a potent oxidant ($(NH_4)_2S_2O_8$) to deeply oxidize the $S_2O_3^{2-}$ to sulfate to improve the oxidation efficiency and reduce the dosage of the $(NH_4)_2S_2O_8$ oxidant. First, the oxidation characteristics of $S_2O_3^{2-}$ and SO_3^{2-} under the action of O_2 and $(NH_4)_2S_2O_8$ were studied using thermodynamic calculations and simulated solutions. Then the influence of various reaction factors in the new technology on the removal rates of $S_2O_3^{2-}$ and SO_3^{2-} in the real desulfurization solution was studied, and the ammonium sulfate product obtained was characterized. The advantages of this new technology were discussed concerning the removal rate and cost of the oxygen−ammonium persulfate and ammonium persulfate alone methods.

2 Experimental

2.1 Materials

Ammonium thiosulfate (60 wt.%), ammonium sulfite monohydrate (90 wt.%), ammonium persulfate (AR grade), manganese dioxide powder (AR grade), ammonia (AR grade) and pure oxygen (99.9%) were used in this study. Ammonium thiosulfate and ammonium sulfite monohydrate were purchased from Shanghai Aladdin Biochemical Technology Co., Ltd. Ammonium persulfate, manganese dioxide powder (AR grade, >99 wt.%, particle size 0.0075 mm) and ammonia were purchased from Tianjin Zhiyuan Chemical Reagent Co., Ltd. Pure oxygen was purchased from Kunming Gas Plant, China.

In the simulated solution experiment, since the concentrations of $S_2O_3^{2-}$ and SO_3^{2-} in the real abnormal desulfurization solution varied in the range of 12−50 and 30−64 g/L, the average concentrations of 30.87 and 46.84 g/L for $S_2O_3^{2-}$ and SO_3^{2-}, respectively, were considered for the preparation of the simulated solution. This solution was used as the source of oxygen oxidation treatment. The solution obtained after oxygen

treatment under optimum conditions was used with ammonium persulfate treatment.

In the real solution experiments, a real abnormal desulfurization solution with high $S_2O_3^{2-}$ and SO_3^{2-} concentrations ($S_2O_3^{2-}$ 48.76 g/L, SO_3^{2-} 61.76 g/L and SO_4^{2-} 176 g/L) provided by a metallurgy company in Yunnan province, China, was used to verify the effect of the oxygen−ammonium persulfate multistage oxidation method. The abnormal desulfurization solution is similar in appearance and pH to the standard desulfurization mother solution, which is a colorless transparent liquid with pH of 5. The difference is that its $S_2O_3^{2-}$ concentration is higher than the upper limit concentration of 3 g/L in the standard desulfurization solution.

2.2 Experimental procedure

In the oxygen oxidation step, 250 mL of the desulfurization solution was transferred to a 1000 mL flask and heated in a water bath. When the temperature of the desulfurization solution reached the set temperature, a certain amount of MnO_2 catalyst was added to the solution. Then, oxygen at a fixed flow rate was passed through the solution using a rubber tube with an aeration stone while stirring at 300 r/min. 5 mL of the oxidized desulfurization solution was used to measure the concentrations of $S_2O_3^{2-}$ and SO_3^{2-} by iodometric methods [17,18]. The removal rates of $S_2O_3^{2-}$ and SO_3^{2-} were calculated using the following equation:

$$R=\frac{C_{\text{ini}}-C_{\text{act}}}{C_{\text{ini}}}\times 100\% \quad (1)$$

where R is the removal rate of $S_2O_3^{2-}$ and SO_3^{2-} under certain conditions, C_{ini} is the initial concentration of $S_2O_3^{2-}$ and SO_3^{2-}, and C_{act} is the actual concentration of $S_2O_3^{2-}$ and SO_3^{2-} under certain conditions.

In the ammonium persulfate oxidation step, the oxygen-oxidized solution (100 mL) was transferred to a 300 mL beaker and heated in a water bath. When the temperature of the desulfurization solution reached the set temperature, a certain amount of ammonium persulfate powder was added to the desulfurization solution, and the oxidation reaction was carried out with stirring at 300 r/min. The oxidized desulfurization solution was collected, and the contents of $S_2O_3^{2-}$ and SO_3^{2-} were measured. The obtained solution was neutralized to pH 8 by adding ammonia, evaporated and crystallized at 85 °C, separated by filtration and then dried at 60 °C for 5 h to obtain ammonium sulfate products. The experiments in the simulated and real desulfurization solutions were all performed as described above. The experiments under the same conditions were carried out 3 times, and the average of the three experiments was taken as the final result. The removal rates of $S_2O_3^{2-}$ and SO_3^{2-} were calculated using the same method in the oxygen oxidation step.

3 Results and discussions

3.1 Oxidation characteristics of $S_2O_3^{2-}$ and SO_3^{2-} under action of oxygen and ammonium persulfate from thermodynamic calculations

3.1.1 Oxygen

The results of thermodynamic calculations of $S_2O_3^{2-}$ and SO_3^{2-} oxidized by oxygen for 1 mol $S_2O_3^{2-}$ and 1 mol SO_3^{2-} or 1 mol oxidant are shown in Fig. 1 from HSC chemistry 6. The Gibbs free energy of each substance in the reaction at different temperatures was obtained from the database of HSC chemistry 6. The reactions of O_2, $S_2O_3^{2-}$ and SO_3^{2-} are shown as

$$S_2O_3^{2-}+2O_2+H_2O=2SO_4^{2-}+2H^+ \quad (2)$$

$$SO_3^{2-}+0.5O_2=SO_4^{2-} \quad (3)$$

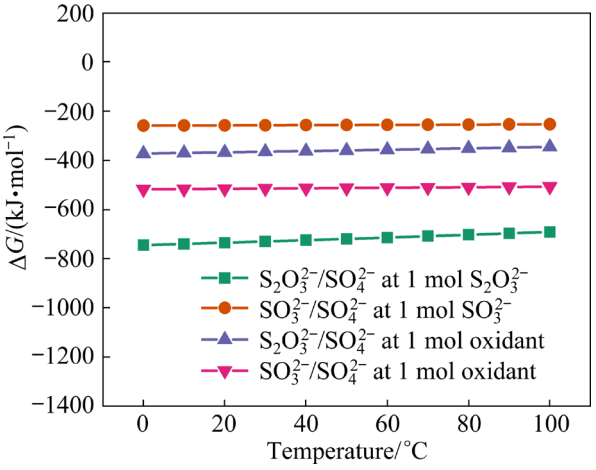

Fig. 1 Thermodynamic calculation results of $S_2O_3^{2-}$ and SO_3^{2-} oxidized by oxygen for 1 mol $S_2O_3^{2-}$, 1 mol SO_3^{2-} and 1 mol oxidant

For 1 mol $S_2O_3^{2-}$ and 1 mol SO_3^{2-}, the Gibbs free energy of the oxidation of $S_2O_3^{2-}$ by oxygen is lower than that of SO_3^{2-}, which means that oxygen

is more likely to react with $S_2O_3^{2-}$ than with SO_3^{2-} when the concentrations of $S_2O_3^{2-}$ and SO_3^{2-} are the same, and O_2 is sufficient from the thermodynamic point of view. However, at 1 mol oxygen, it is found that the Gibbs free energy of the oxidation of SO_3^{2-} by oxygen is lower than that of $S_2O_3^{2-}$, indicating that oxygen tends to react with SO_3^{2-} rather than $S_2O_3^{2-}$ under insufficient oxygen conditions. This phenomenon can be explained by Reactions (2) and (3); the oxidant oxygen required for SO_3^{2-} is 1/4 of that required for $S_2O_3^{2-}$, and hence SO_3^{2-} is more likely to react with oxygen than $S_2O_3^{2-}$ when the oxidant is insufficient. Therefore, according to the thermodynamic calculations, the removal rate of oxygen on $S_2O_3^{2-}$ is better than that on SO_3^{2-} under conditions of sufficient oxygen, while the opposite is true under conditions of insufficient oxygen.

3.1.2 Ammonium persulfate

The results of thermodynamic calculations of $S_2O_3^{2-}$ and SO_3^{2-} oxidized by ammonium persulfate 1 mol of $S_2O_3^{2-}$ and 1 mol SO_3^{2-}, or 1 mol of oxidants are shown in Fig. 2 from HSC chemistry 6.

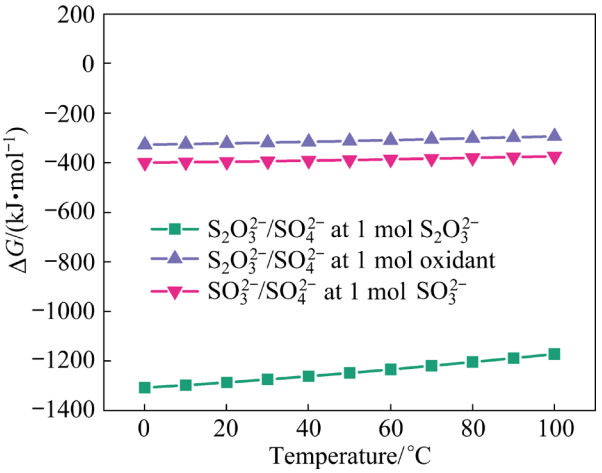

Fig. 2 Thermodynamic calculation results of $S_2O_3^{2-}$ and SO_3^{2-} oxidized by ammonium persulfate for 1 mol $S_2O_3^{2-}$, 1 mol SO_3^{2-} and 1 mol oxidant

The reactions of $S_2O_8^{2-}$, $S_2O_3^{2-}$ and SO_3^{2-} are shown as

$$S_2O_8^{2-}+0.25S_2O_3^{2-}+1.2H_2O=2.5SO_4^{2-}+2.5H^+ \quad (4)$$

$$S_2O_8^{2-}+SO_3^{2-}+H_2O=3SO_4^{2-}+2H^+ \quad (5)$$

As shown in Fig. 2, $S_2O_8^{2-}$ has similar oxidation reaction characteristics with $S_2O_3^{2-}$ and SO_3^{2-} as oxygen thermodynamically, i.e., it is more prone to react with $S_2O_3^{2-}$ under sufficient oxidant conditions and more prone to react with SO_3^{2-} in the case of insufficient oxidant.

When the oxidant is insufficient to convert both $S_2O_3^{2-}$ and SO_3^{2-} into SO_4^{2-}, the difference in Gibbs free energy of O_2 oxidizing $S_2O_3^{2-}$ and SO_3^{2-} (~130 kJ/mol) is greater than that of $S_2O_8^{2-}$ oxidizing $S_2O_3^{2-}$ and SO_3^{2-} (~90 kJ/mol). However, the difference in Gibbs free energy of $S_2O_8^{2-}$ oxidizing $S_2O_3^{2-}$ and SO_3^{2-} (800−900 kJ/mol) is greater than that of O_2 oxidizing $S_2O_3^{2-}$ and SO_3^{2-} (450−500 kJ/mol) under sufficient oxidant conditions. This shows that the difference in the oxidation characteristics of SO_3^{2-} and $S_2O_3^{2-}$ under oxygen is greater than that under ammonium persulfate in the initial stage of the oxidation reaction (insufficient oxidant). In contrast, the difference in the oxidation characteristics of SO_3^{2-} and $S_2O_3^{2-}$ under ammonium persulfate is more significant than that under oxygen in the latter stage of the reaction (sufficient oxidant). Therefore, to reduce the addition of ammonium persulfate oxidant, it is thermodynamically feasible to oxidize most of the sulfite with oxygen and then oxidize the remaining $S_2O_3^{2-}$ and SO_3^{2-} with ammonium persulfate.

3.2 Effect of oxygen−ammonium persulfate multistage oxidation in simulated desulfurization solution

3.2.1 Oxygen oxidation

(1) Effect of MnO_2 catalyst

MnO_2 was used as a catalyst in our work to improve the oxygen removal rate due to its stability in alkaline to weakly acidic conditions, low solubility in water, hard texture, not easily broken by mechanical stirring. In addition, the price of MnO_2 is lower than that of other noble metal catalysts [19,20]. Experiments to investigate the effect of the MnO_2 catalyst were carried out at room temperature (20 °C) for different reaction time (1−6 h) with an oxygen intake of 0.8 L/min, and an initial pH of 7. The removal rates of $S_2O_3^{2-}$ and SO_3^{2-} when the simulated desulfurization solution was oxidized by oxygen without catalyst are shown in Fig. 3(a), and the results when 0.5 g/L MnO_2 was added are shown in Fig. 3(b).

The addition of MnO_2 catalyst can promote oxygen oxidation of SO_3^{2-} but not $S_2O_3^{2-}$. The removal rate of SO_3^{2-} by oxygen for 3 h increases from 36.71% to 76.08% after the addition of 0.5 g/L MnO_2 catalyst (Fig. 3(b)), while the removal rate of

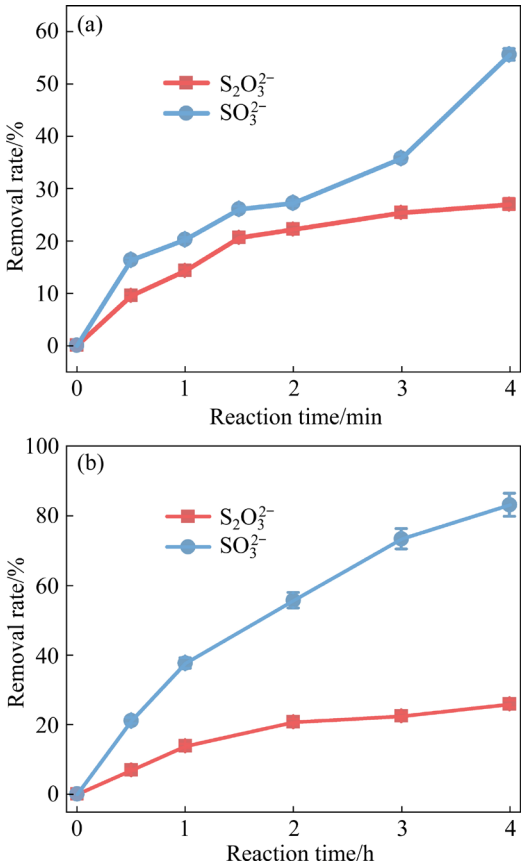

Fig. 3 Removal rates of $S_2O_3^{2-}$ and SO_3^{2-} oxidized by oxygen without (a) and with (b) MnO_2 catalyst

$S_2O_3^{2-}$ remains at 23.8% with and without catalyst (Fig. 3(a)). These results can be attributed to the thermodynamics of SO_3^{2-}, which reacts more readily with oxygen than with $S_2O_3^{2-}$ under insufficient oxidant and high concentration of SO_3^{2-}, as shown in Section 3.1.1. Another reason why $S_2O_3^{2-}$ cannot accelerate the reaction under catalytic conditions is that the reaction of $S_2O_3^{2-}$ with oxygen is a zero-order reaction [21,22], which means that the reaction is not affected by the concentration of $S_2O_3^{2-}$ [23,24]. By comparing the mass of MnO_2 catalyst before and after the reaction, it is found that the loss of catalyst mass is less than 0.5%; that is, there is almost no residual manganese in the solution. The error in the removal rate of SO_3^{2-} and $S_2O_3^{2-}$ by the MnO_2 catalyst is still within 3% after three cycles of experiments, indicating that the MnO_2 catalyst used in our work has good reusability and stability.

SEM images and spot scanning by SEM−EDS of the MnO_2 catalyst before and after oxidation were investigated by using a scanning electron microscope (Philips XL20 ESEM-TMP, Amsterdam, Netherlands), as shown in Fig. 4. The FTIR spectra of the MnO_2 catalyst before and after oxidation were obtained by using an infrared spectrometer (ALPHA, Bruker, USA), and the results are shown in Fig. 5. The microscopic morphology of MnO_2 (Fig. 4) changes from flat before oxidation to uneven after oxidation. The spot scanning by SEM−EDS of the MnO_2 catalyst also shows that the sulfur-containing components are attached to the surface of the MnO_2 catalyst, proving that the oxidation reactions of SO_3^{2-} and $S_2O_3^{2-}$ occur on the surface of MnO_2. MnO_2 catalyzes oxygen to oxidize SO_3^{2-} and $S_2O_3^{2-}$ by changing its valence state. These different valence states of manganese ($Mn^{(4-n)+}$) react with oxygen and SO_3^{2-} and $S_2O_3^{2-}$ in the solution, thus promoting the oxidation reaction. The following equations can express the main reactions of MnO_2 changing different valence states:

$$Mn^{4+}+SO_3^{2-}/S_2O_3^{2-}\rightarrow SO_4^{2-}+Mn^{(4-n)+} \quad (6)$$

$$Mn^{(4-n)+}+O_2+H_2O\rightarrow OH^-+Mn^{4+} \quad (7)$$

The FTIR spectra (Fig. 5) of the catalyst samples before and after oxidation show obvious

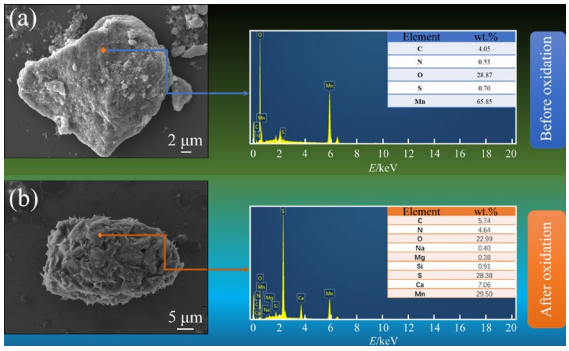

Fig. 4 SEM images and spot scanning results by SEM−EDS of MnO_2 catalyst before (a) and after (b) oxidation

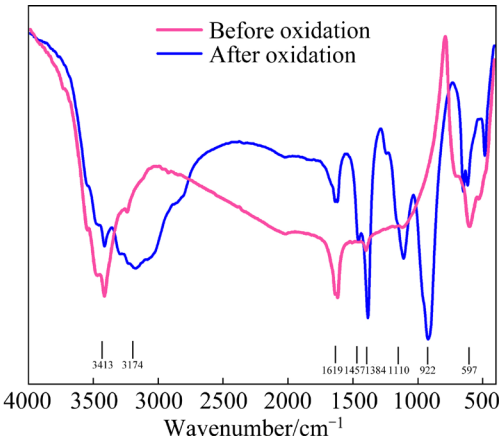

Fig. 5 FTIR spectra of MnO_2 catalyst

peaks at 3413, 3174, 1619 and 1384 cm^{-1}. Among them, the former two are caused by the O—H vibrating mode of traces of the absorbed water [25], while the latter two are caused by the bending and stretching of H—O—H in the crystal water. The peaks around 597 cm^{-1} correspond to the Mn—O stretching vibration [26]. Different from the FTIR spectra of the catalyst sample before oxidation, there are significant peaks at around 1110 and 922 cm^{-1} in the FTIR spectra of the catalyst sample after oxidation, attributed to the metal—oxygen (Mn—O) bending vibrations of [MnO_6] [27]. This result further confirms that the catalytic mechanism of MnO_2, as shown in Reactions (5) and (6), is accurate. In addition, the peaks at around 1457, 1384 and 1110 cm^{-1} in the FTIR spectra of the catalyst sample after oxidation were also reported to be deformed by SO_4^{2-}, SO_3^{2-} and $S_2O_3^{2-}$ deformation vibrations of $(NH_4)_2SO_4$, $(NH_4)_2SO_3$ and $(NH_4)_2S_2O_3$ [28].

In addition, under the action of MnO_2 catalyst, prolonging the reaction time can obviously promote the oxidation of SO_3^{2-}, but its promoting effect on the oxidation of $S_2O_3^{2-}$ is relatively weak, as shown in Fig. 3(b). There is an obvious effect on the removal rate of SO_3^{2-} within 3 h, and the SO_3^{2-} concentration in the simulated solution after oxidation for 3 h is 14.21 g/L, which is lower than that (≤15 g/L) in the relevant production standard. Therefore, 3 h is selected as the appropriate oxidation time for the subsequent experiments.

(2) Effect of reaction temperature

Experiments to investigate the effect of reaction temperature were carried out at different temperatures (20, 40, 50 and 60 °C) for 3 h with oxygen intake of 0.8 L/min and initial pH of 7, and the result is shown in Fig. 6(a).

The removal rates of $S_2O_3^{2-}$ and SO_3^{2-} increase from 76.08% to 97.25% and from 23.83% to 27.37%, respectively, as the temperature increases from 20 to 50 °C, and then there is no noticeable change in the removal rate after 50 °C. This may be due to the fact that the reaction rate increases steadily with increasing temperature, while the solubility of oxygen in aqueous decreases. The oxygen solubility in water decreases with increasing temperature: 0.0700 g/L at 0 °C, 0.0300 g/L at 50 °C, and 0.0280 g/L at 60 °C. Therefore, 50 °C is chosen as the optimum reaction temperature based on the removal effect of SO_3^{2-} at different temperatures and the actual temperature of the desulfurization solution, which ranges from 40 to 50 °C.

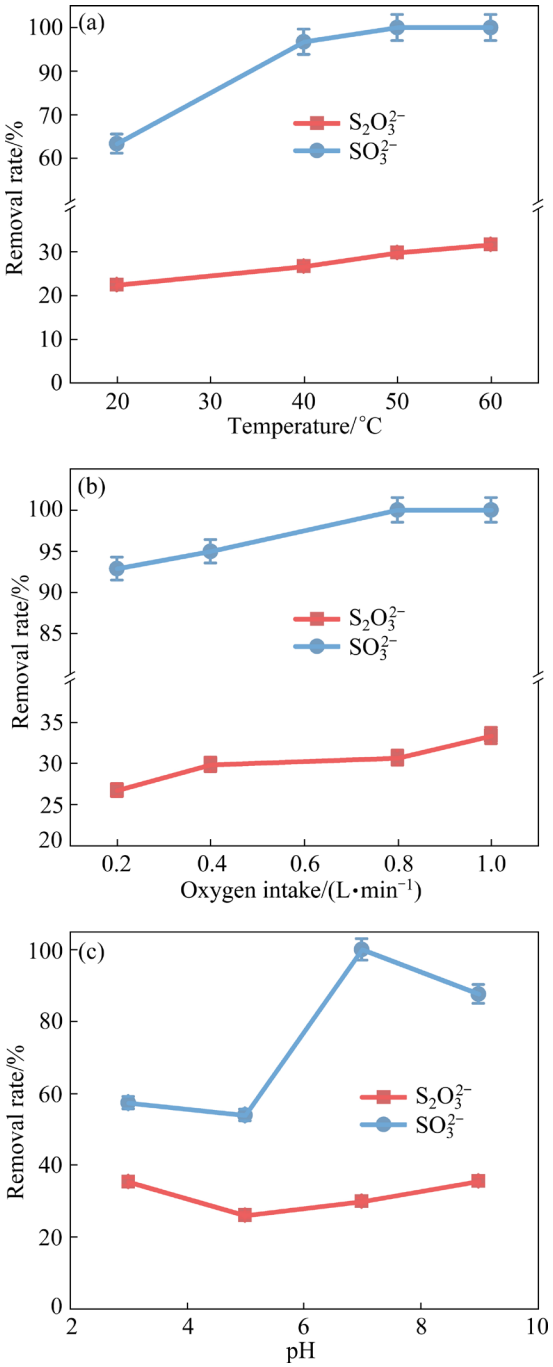

Fig. 6 Effect of reaction temperature (a), oxygen intake (b) and pH (c) on removal rate in oxygen oxidation step

(3) Effect of oxygen intake

Experiments to investigate the effect of oxygen intake were carried out under different oxygen intakes (0.2, 0.4, 0.8 and 1.0 L/min) at 50 °C for 3 h with initial pH of 7, and the result is shown in Fig. 6(b).

Increasing the oxygen intake is beneficial to the oxidation of SO_3^{2-} and $S_2O_3^{2-}$. The removal rates of both $S_2O_3^{2-}$ and SO_3^{2-} increased from 92.85 to 97.25% and from 26.29 to 27.37%, respectively, as the oxygen intake increased from 0.2 to 0.8 L/min. However, the effect of oxygen intake on the oxidation of $S_2O_3^{2-}$ and SO_3^{2-} is not apparent after the oxygen intake reaches 0.8 L/min. Oxygen has a low solubility in water; therefore, excessive oxygen intake causes more oxygen to escape and be wasted. Therefore, the oxygen intake is consequently considered to be 0.8 L/min.

(4) Effect of pH

Experiments to investigate the effect of pH value were carried out under different initial pH (3, 5, 7 and 9) at 50 °C for 3 h with an oxygen intake of 0.8 L/min, and the result is shown in Fig. 6(c).

The removal rates of $S_2O_3^{2-}$ and SO_3^{2-} are optimal with a solution pH of 7, indicating that maintaining the pH at neutral level favors the oxidation of SO_3^{2-}. These results can be explained by the dissolution of the MnO_2 catalyst under acidic conditions and the instability of the sulfur-containing intermediates produced by the oxidation process under alkaline conditions. The MnO_2 catalyst is observed to dissolve immediately at pH 3, while at pH 5, it begins to dissolve after about 2 h, and the catalyst is not observed at 2.5 h. Therefore, the decomposition of the catalyst under acidic conditions is the direct cause of the decrease in the reaction rate. On the other hand, the decrease in the oxidation rate of $S_2O_3^{2-}$ under alkaline conditions can be attributed to the instability of intermediates under alkaline conditions. In agreement with the work of ZELINSKII and NOVGORODTSEVA [29], SO_3^{2-} is oxidized to generate hyposulfite ($S_2O_6^{2-}$), in which the valence state of the sulfur ion is +5 under insufficient oxidant. The hyposulfite is unstable under alkaline conditions and decomposes into SO_3^{2-} and SO_3^{2-}. The main reaction for the decomposition of $S_2O_6^{2-}$ into SO_3^{2-} and SO_4^{2-} can be expressed by

$$S_2O_6^{2-}+2OH^-=SO_3^{2-}+SO_4^{2-}+H_2O \quad (8)$$

Therefore, the optimum solution of pH 7, is chosen as the optimum condition of the simulation experiment.

In summary, the optimal conditions for oxygen oxidation are achieved at 50 °C for 3 h with an oxygen intake of 0.8 L/min, a simulated solution volume of 250 mL, an initial pH of 7, and stirring at 300 r/min. Under these conditions, the $S_2O_3^{2-}$ concentration decreased from 30.87 to 22.42 g/L, the SO_3^{2-} concentration decreased from 46.84 to 1.29 g/L, and the pH of the treated solution was 5.

3.2.2 Ammonium persulfate oxidation

The simulated solution obtained after oxygen treatment under optimal conditions was treated with ammonium persulfate. The concentrations of $S_2O_3^{2-}$ and SO_3^{2-} in the mother solution after oxygen oxidation under the optimized conditions are 22.42 and 1.29 g/L, respectively. After oxygen oxidation, the pH of desulfurization solution is decreased from 7 to 5.

(1) Effect of pH

Experiments to investigate the effect of the pH on the ammonium persulfate oxidation step were carried out under different pH (3, 5, 7 and 9) at 50 °C for 10 min with the addition of 80 g/L ammonium persulfate to the solution, and the result is shown in Fig. 7(a).

The oxidation efficiency of $S_2O_3^{2-}$ and SO_3^{2-} decreases with increasing pH, especially under alkaline conditions. Theoretically, 185 g/L ammonium persulfate is needed to completely oxidize 22.42 g/L $S_2O_3^{2-}$ and 1.29 g/L SO_3^{2-} into SO_4^{2-}. The amount of ammonium persulfate added is only 80 g/L, but most of $S_2O_3^{2-}$ and SO_3^{2-} have been removed, which means that some intermediates, such as tetrathionate ($S_4O_6^{2-}$) and trithionate ($S_3O_6^{2-}$), are produced, as mentioned in Ref. [30]. The tetrathionate and trithionate can be easily decomposed into $S_2O_3^{2-}$ and SO_3^{2-} under alkaline conditions, as shown by the following equations [31]:

$$S_4O_6^{2-}+3OH^-=1.5S_2O_3^{2-}+SO_3^{2-}+1.5H_2O \quad (9)$$

$$2S_3O_6^{2-}+6OH^-=S_2O_3^{2-}+4SO_3^{2-}+3H_2O \quad (10)$$

Therefore, the decrease in $S_2O_3^{2-}$ and SO_3^{2-} removal rates with increasing pH can be attributed to the decomposition of unstable intermediates with increasing pH. Optimum $S_2O_3^{2-}$ and SO_3^{2-} removal rates are achieved at pH of 3−5. Considering that the pH of the solution after the oxygen oxidation step is just 5 under the optimum condition, it is taken as the optimum pH condition for the ammonium persulfate oxidation step.

(2) Effect of reaction time

Experiments to investigate the effect of reaction time on the ammonium persulfate

oxidation step were carried out under different reaction time (3, 5, 8, 10, and 20 min) at 50 °C with 80 g/L ammonium persulfate and pH of 5, and the result is shown in Fig. 7(b).

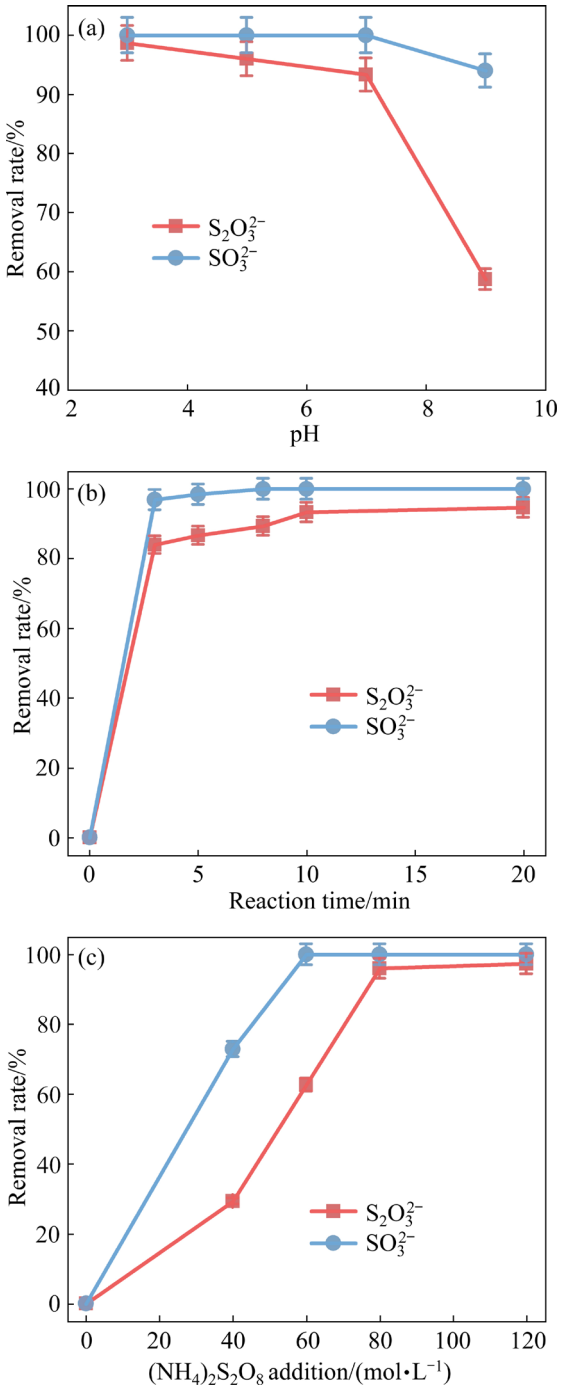

Fig. 7 Effect of pH (a), reaction time (b), and $(NH_4)_2S_2O_8$ addition (c) on removal rate in ammonium persulfate oxidation step

As shown in Fig. 7(b), extending time promotes the oxidation of $S_2O_3^{2-}$ and SO_3^{2-}. The reaction between ammonium persulfate and the desulfurization solution is almost completed within 10 min, with $S_2O_3^{2-}$ removal rate of 96.1% and SO_3^{2-} removal rate of 99.7%. This is due to the advantages of the high solubility and strong oxidizing property of ammonium persulfate [15]. Therefore, the optimum reaction time in the ammonium persulfate oxidation step is 10 min.

(3) Effect of $(NH_4)_2S_2O_8$ addition

Experiments to investigate the effect of $(NH_4)_2S_2O_8$ addition in ammonium persulfate oxidation step were carried out with different $(NH_4)_2S_2O_8$ additions (40, 60, 80, and 120 g/L) at 50 °C for 10 min and pH of 5, and the result is shown in Fig. 7(c).

Increasing the addition of $(NH_4)_2S_2O_8$ benefits the oxidation of $S_2O_3^{2-}$ and SO_3^{2-}, which significantly increases the removal rates of $S_2O_3^{2-}$ and SO_3^{2-}. However, the removal rates of $S_2O_3^{2-}$ and SO_3^{2-} both reached over 96% after the $(NH_4)_2S_2O_8$ addition reached 80 g/L, and increased slowly when the $(NH_4)_2S_2O_8$ addition was further increased. This may be because $S_2O_3^{2-}$ and SO_3^{2-} are completely converted to SO_4^{2-} or other intermediates when 80 g/L $(NH_4)_2S_2O_8$ is added. Therefore, 80 g/L is chosen as the optimum $(NH_4)_2S_2O_8$ addition.

In summary, based on the simulated solution experiments, the optimal conditions for the ammonium persulfate oxidation step are as follows: 50 °C reaction temperature, 10 min reaction time, 80 g/L $(NH_4)_2S_2O_8$ addition, 100 mL simulated mother solution, pH 5, and 300 r/min mixing rate. Under these conditions, the $S_2O_3^{2-}$ content decreased from 22.42 to 1.21 g/L, and the SO_3^{2-} content decreased from 1.29 to 0.18 g/L. After oxygen−ammonium persulfate multistage oxidation, the oxidation rates of $S_2O_3^{2-}$ and SO_3^{2-} in the simulated desulfurization solution are 96.1% and 99.7%, respectively, which is remarkable.

3.3 Effect of oxygen−ammonium persulfate multistage oxidation on real desulfurization solution

An abnormal real desulfurization solution containing 48.76 g/L $S_2O_3^{2-}$, 61.76 g/L SO_3^{2-}, and 176 g/L SO_4^{2-} was used in this experiment. The effect of oxygen on the real desulfurization solution was investigated under the optimum oxidation conditions of oxygen for the simulated desulfurization solution, i.e., 50 °C reaction

temperature with an oxygen intake of 0.8 L/min, a solution pH of 7, a desulfurization solution volume of 250 mL, 0.5 g/L MnO_2 addition, and a mixing rate of 300 r/min. The pH of the real solution was adjusted from an initial pH of 5−7 using ammonia. The removal rates of $S_2O_3^{2-}$ and SO_3^{2-} when the real desulfurization solution was oxidized by oxygen with the addition of 0.5 g/L MnO_2 are shown in Fig. 8.

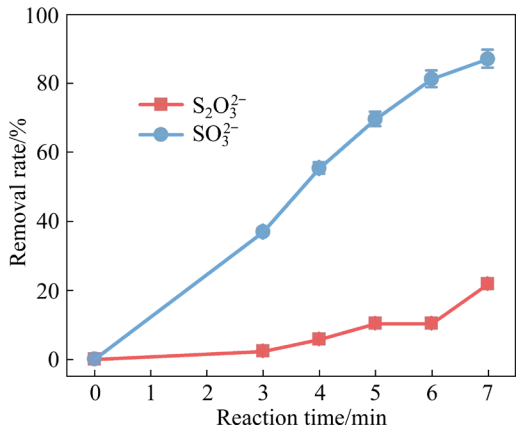

Fig. 8 Effect of removal rate of oxygen oxidation step on real desulfurization solution

The extension of the reaction time of the oxygen oxidation step is beneficial for the oxidation of SO_3^{2-} in the real solution, while the effect on $S_2O_3^{2-}$ is not significant. The oxidation characteristics of $S_2O_3^{2-}$ and SO_3^{2-} in the real solution under oxygen oxidation are similar to those in the simulated solution. The difference is that the oxidation rates of $S_2O_3^{2-}$ and SO_3^{2-} in the real solution are not as high as those in the simulated solution under the same conditions. This is because the sulfate concentration in the real solution is high (176 g/L), which reduces the solubility and mass transfer rate of oxygen [32]. As a result, it takes only 3 h for the SO_3^{2-} concentration in the simulated solution to reach the industrially required residual SO_3^{2-} concentration (<15 g/L), while it takes 6 h in the real solution. The concentration of $S_2O_3^{2-}$ decreased from 48.76 to 38.11 g/L, and the concentration of SO_3^{2-} decreased from 61.76 to 17.61 g/L in the real desulfurization solution after oxidation by oxygen at 50 °C for 6 h.

Then, the real solution obtained after the above oxygen oxidation step is subjected to ammonium persulfate oxidation. The $(NH_4)_2S_2O_8$ oxidation experiment on the real solution was carried out under the optimum oxidation conditions of $(NH_4)_2S_2O_8$ for the simulated desulfurization solution, which is at 50 °C for 10 min with a solution volume of 100 mL, a solution pH of 5 and under stirring at 300 r/min. The experimental results show that the oxygen−ammonium persulfate multistage oxidation method can greatly oxidize and remove $S_2O_3^{2-}$ and SO_3^{2-} in real absorption solutions. After the ammonium persulfate oxidation step, a real desulfurization solution is obtained containing 2.24 g/L $S_2O_3^{2-}$ and 0.02 g/L SO_3^{2-} with a final pH of 4. In other words, when the oxygen−ammonium persulfate multistage oxidation method is used to treat the real desulfurization solution with a high concentration of $S_2O_3^{2-}$, the removal rates of $S_2O_3^{2-}$ and SO_3^{2-} are as high as 95.4% and 99.97%, respectively.

3.4 Comparison of sulfuric acid, ammonium persulfate alone, and oxygen−ammonium persulfate multistage oxidation

3.4.1 Removal rate

The effect of the ammonium persulfate method was studied under the same optimum conditions as the oxygen−ammonium persulfate method i.e., at 50 °C for 10 min with a real desulfurization solution volume of 100 mL, a solution pH of 5 and stirring at 300 r/min, except that the addition of $(NH_4)_2S_2O_8$ added was changed to 120, 140, 160, and 180 g/L. The removal rates of $S_2O_3^{2-}$ and SO_3^{2-} when the real desulfurization solution was oxidized by ammonium persulfate alone are shown in Fig. 9.

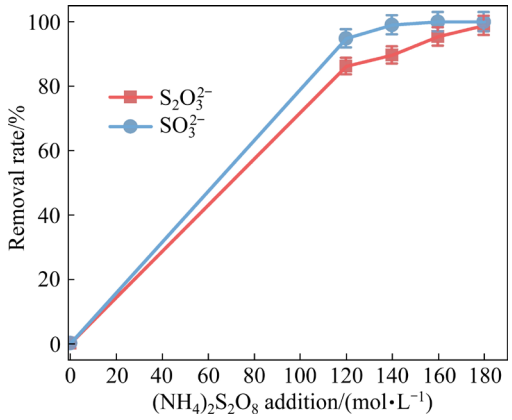

Fig. 9 Effect of removal rate of ammonium persulfate alone on real desulfurization solution

The concentrations of $S_2O_3^{2-}$ and SO_3^{2-} are 2.24 and 0.02 g/L, respectively, when 160 g/L ammonium persulfate alone is added, as shown in

Fig. 9, achieving the same removal rate by the oxygen−ammonium persulfate method. That is, the oxygen−ammonium persulfate method requires only half the addition of oxidant, 80 g/L, compared to the ammonium persulfate alone approach with 160 g/L ammonium persulfate. In addition, SO_3^{2-} in solution reacts with ammonium persulfate to release the proton H^+, which does not occur when it reacts with oxygen, as shown in Eqs. (4) and (6). As a result, the decrease in the pH of the solution obtained by the ammonium persulfate alone is greater than that of the oxygen−ammonium persulfate oxidation. The final pH of the real solution after oxidation by using $(NH_4)_2S_2O_8$ alone method is 2 at this point, while that in the case of oxygen−ammonium persulfate method is 4. This means that the neutralization step of the ammonium persulfate alone consumes more ammonia than the neutralization step by oxygen−ammonium persulfate, which can reduce the treatment cost.

The chromaticity, XPS, XRD and SEM results of the ammonium sulfate products obtained by the traditional concentrated sulfuric acid process, ammonium persulfate process, and oxygen-ammonium persulfate process are shown in Figs. 10−13. Among them, XPS, XRD and SEM results were obtained from PHI−5300, Rigaku dX 2000, and Philips XL20 ESEM-TMP instruments, respectively.

The chromaticity of the solid products obtained using oxygen−ammonium persulfate oxidation (Fig. 10(a)) and ammonium persulfate oxidation (Fig. (b)) is white, which is different from the yellow product obtained by the traditional concentrated sulfuric acid process (Fig. 10(c)).

The XPS spectra in Figs. 11(a) and (b) show that the dominant peaks of sulfate (SO_4^{2-}) and tetrathionate ($S_4O_6^{2-}$) are around 168.3 and 163.8 eV [33,34], respectively, for multistage oxidation and ammonium persulfate oxidation alone. However, the XPS spectrum in Fig. 11(c) has a wide range of peaks with binding energies in the range of 161−166 eV that can be fitted to a combination of sulfur (S_0) and $S_4O_6^{2-}$ [33], confirming the presence of sulfur impurities (S_0) in the yellow product obtained by sulfuric acid oxidation.

Fig. 10 Chromaticity of $(NH_4)_2SO_4$ products oxidized by oxygen−ammonium persulfate (a), ammonium persulfate (b), and concentrated sulfuric acid (c)

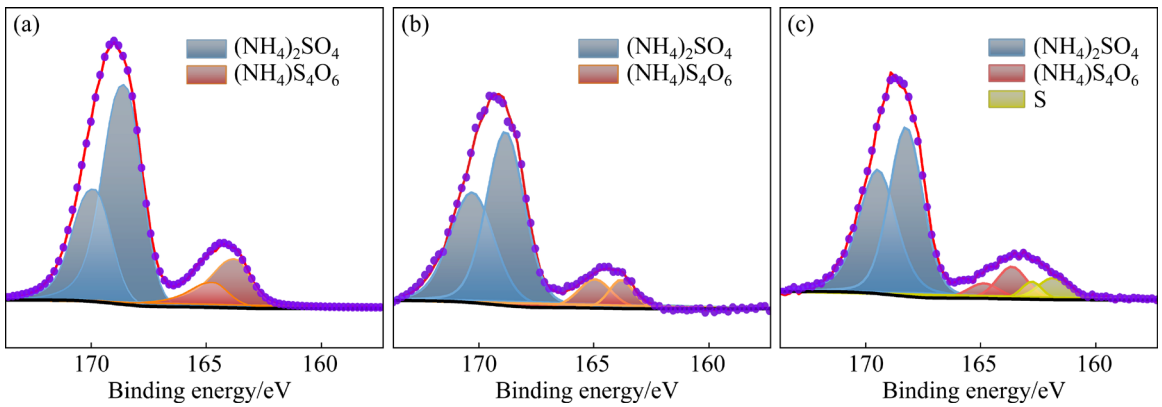

Fig. 11 XPS spectra of $(NH_4)_2SO_4$ products oxidized by oxygen−ammonium persulfate (a), ammonium persulfate (b), and concentrated sulfuric acid (c)

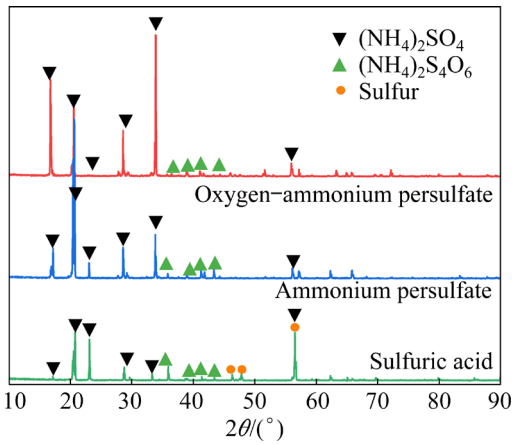

Fig. 12 XRD patterns of solid products obtained by concentrated oxygen−ammonium persulfate, ammonium persulfate, and sulfuric acid oxidation

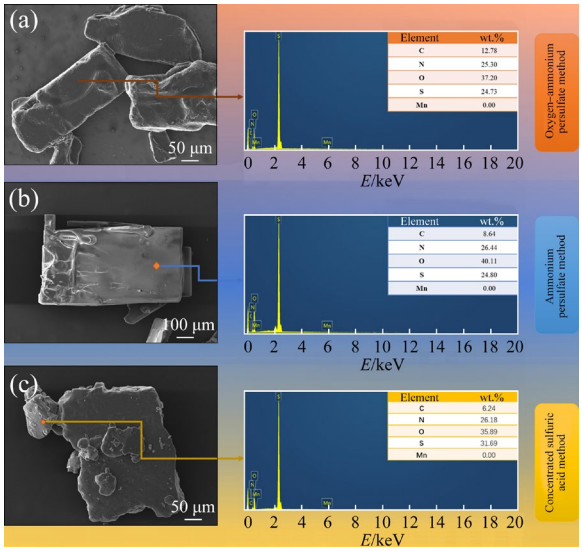

Fig. 13 SEM images and spot scanning results of $(NH_4)_2SO_4$ products by oxygen−ammonium persulfate (a), ammonium persulfate (b), and concentrated sulfuric acid (c)

In addition, the height ratios of the SO_4^{2-} peak to the $S_4O_6^{2-}$ peak of the solid product by the oxygen−ammonium persulfate oxidation process and the ammonium persulfate alone process are 1:0.28 and 1:0.18, respectively, which means that more intermediate products ($S_4O_6^{2-}$) are formed by the oxygen−ammonium persulfate oxidation. The reason for this phenomenon is that the oxidation ability of oxygen by the multistage oxidation is not as strong as that of ammonium persulfate by ammonium persulfate alone.

The XRD results (Fig. 12) show that weak diffraction peaks of sulfur are detected in the ammonium sulfate product obtained by the traditional concentrated sulfuric acid oxidation method, but not in the products by the multistage oxidation and ammonium persulfate alone oxidation methods.

The SEM images in Fig. 13 show that the product obtained by the oxygen−ammonium persulfate oxidation process has larger and more average crystal shapes than the product formed by the traditional concentrated sulfuric acid oxidation process.

The spot scanning results in Fig. 13 show that manganese dioxide was not found in the product produced by the oxygen−persulfate method, indicating that the multi-stage oxidation method did not introduce new impurities into the product. In addition, the product obtained by the oxygen−ammonium persulfate method has a lower sulfur content than that obtained from the traditional concentrated sulfuric acid oxidation process. The excess sulfur on the product's surface in the traditional concentrated sulfuric acid oxidation process may be due to sulfur impurities, which are responsible for the abnormal color of ammonium sulfate products. And no manganese is found in multiple locations in the product.

In summary, compared with the traditional concentrated sulfuric acid oxidation method, the multistage oxidation method can solve the abnormal chromaticity problem of ammonium sulfate products when oxidizing the desulfurization solution with a high concentration of $S_2O_3^{2-}$. Compared with the ammonium persulfate alone, the multistage oxidation can also reduce the addition of ammonium persulfate and ammonia on the basis of obtaining a qualified chromaticity of ammonium sulfate products.

The difference in removal rates between this work and other recent studies of $S_2O_3^{2-}$ and SO_3^{2-} oxidation is compared in Table 1. As shown, the multistage oxidation method in this work has certain advantages in the removal rates of $S_2O_3^{2-}$ and SO_3^{2-} compared with other studies. In addition, the multistage oxidation method provided in our work can effectively treat solutions containing high concentrations of $S_2O_3^{2-}$ and SO_3^{2-}, especially mixed solutions of $S_2O_3^{2-}$ and SO_3^{2-} under mild conditions of atmospheric pressure and low temperature, thereby solving the problems of only treating solutions of single components with low concentrations of $S_2O_3^{2-}$ and SO_3^{2-} and requiring high temperature and high pressure in existing processes.

Table 1 Comparison in removal rates of $S_2O_3^{2-}$ and SO_3^{2-}

Oxidized object	Oxidation method	Initial concentration/ ($g \cdot L^{-1}$)	Removal rate/%	Source
SO_3^{2-}	Oxygen	28	98.1	[35]
SO_3^{2-}	Ozone	12.8	98.5	[23]
SO_3^{2-}	Ozone with a rotating packed bed (RPB)	8	97.5	[36]
$S_2O_3^{2-}$	Oxygen with Cu (II) catalyst	1	98.0	[14]
$S_2O_3^{2-}$	Oxygen at 85 °C and 0.6 MPa	0.11	83.9	[37]
$S_2O_3^{2-}$	Air at 230 °C and 6.8 MPa	20	88.9	[38]
SO_3^{2-}	Multistage oxidation	61.76	99.9	This work
$S_2O_3^{2-}$	Multistage oxidation	48.76	95.4	This work

3.4.2 Estimated cost

In addition to studying the removal rate, the cost of the treatment technology is also an essential factor in its viability for industrial application. The quality of the ammonium sulfate product is 296.81 g when using the oxygen−ammonium persulfate process and 370.67 g when using the ammonium persulfate process, found by considering the volume of the absorbed desulfurization solution as 1 L. Since the dosage of ammonium persulfate added in the ammonium persulfate alone process is significantly higher than that in the oxygen−ammonium persulfate oxidation process, more ammonium persulfate is converted into an ammonium sulfate product. In other words, to produce 1 t of ammonium sulfate, the ammonium persulfate consumption required by the ammonium persulfate process and the oxygen−ammonium persulfate oxidation process is 431.65 and 269.53 kg, respectively. This indicates that the oxygen−ammonium persulfate multistage oxidation process can reduce ammonium persulfate consumption by 37.56% compared with the ammonium persulfate oxidation process alone.

The cost accounting of the oxygen−ammonium persulfate method and ammonium persulfate alone method is carried out considering 1 t of ammonium sulfate production, and the results are shown in Table 2. The cost of oxygen−ammonium persulfate is 28.13% lower than that of ammonium persulfate alone. Using oxygen instead of ammonium persulfate to oxidize SO_3^2 can effectively reduce the treatment cost of the desulfurization solution and result in a qualified ammonium sulfate solid at a low treatment cost.

Table 2 Cost of oxygen−ammonium persulfate and ammonium persulfate processes (US$\cdot t^{-1}$)

Additive	Ammonium persulfate	Oxygen−ammonium persulfate
Oxygen (including stirring electricity)	–	67.55
Ammonium persulfate	295.65	184.82
Ammonia	74.77	49.54
Total	370.42	301.91

4 Conclusions

(1) Thermodynamic calculations revealed the differences in the oxidation characteristics of different oxidants (oxygen and ammonium persulfate) towards $S_2O_3^{2-}$ and SO_3^2. Oxygen had a definite removal effect on SO_3^{2-} in the desulfurization solution, while ammonium persulfate could efficiently oxidize both $S_2O_3^{2-}$ and SO_3^{2-}. Therefore, the order of oxidant addition was determined by adding oxygen first and then ammonium persulfate.

(2) The removal rates of $S_2O_3^{2-}$ and SO_3^{2-} concentrations in the simulated solution were 96.1% and 99.7%, respectively, while those in the real desulfurization solution were 95.4% and 99.97%, respectively. The oxygen−ammonium persulfate multistage oxidation can realize the economical and efficient oxidation of the desulfurization solution.

(3) Compared with other recent studies, the multistage oxidation method can effectively treat solutions containing high concentrations of $S_2O_3^{2-}$ and SO_3^{2-} at atmospheric pressure and low temperature. The multistage oxidation can reduce ammonium persulfate consumption by 37.56% and reduce the treatment cost by 28.13% compared with the ammonium persulfate alone. The same treatment effect, as that of ammonium persulfate alone could be achieved by the oxygen−ammonium persulfate multistage oxidation with a reduced treatment cost.

CRediT authorship contribution statement

Hao-ran XU: Formal analysis, Writing − Original draft; **Wei-chao HUANG:** Formal analysis; **A. V. RAVINDRA** and **Duc-lenh PHAN:** Writing − Review and editing; **Thi-quynh-xuan LE:** Conceptualization, Project administration, Writing − Review and editing; **Li-bo ZHANG** and **Shao-hua YIN:** Resources, Supervision.

Declaration of competing interest

The authors declare that they have no known competing financial interests or personal relationships that could have appeared to influence the work reported in this paper.

Acknowledgments

The authors acknowledge the financial support of the Yunnan Major Scientific and Technological Project, China (No. 202302AG050008), Yunnan Fundamental Research Project, China (No. 202101BE070001-023), and "Yunnan Revitalization Talents Support Plan" High-End Foreign Talents Program, China.

References

[1] LISNIC R, JINGA S I. Study on current state and future trends of flue gas desulphurization technologies: A review [J]. Romanian Journal of Materials, 2018, 48(1): 83−90.

[2] LI Xiao-li, LIU Quan-bo, WANG Kang, WANG Fu-qiang, CUI Gui-mei, LI Yang. Multimodel anomaly identification and control in wet limestone-gypsum flue gas desulphurization system [J]. Complexity, 2020, 2020: 1−17. https://doi.org/10.1155/2020/6046729.

[3] XUE Juan-qin, LI Jing-xian, LU Xi, MAO Wei-bo, WANG Yu-jie, WU Ming. Absorption of sulfur dioxide using membrane and enhancement of desorption with ultrasound [J]. Transactions of Nonferrous Metals Society of China, 2010, 20(5): 930−934. https://doi.org/10.1016/S1003-6326(09)60238-7.

[4] YE Wan-qi, LI Yun-jiao, KONG Long, REN Miao-miao, HAN Qiang. Feasibility of flue-gas desulfurization by manganese oxides [J]. Transactions of Nonferrous Metals Society of China, 2013, 23(10): 3089−3094. https://doi.org/10.1016/S1003-6326(13)62838-1.

[5] WANG Yi, LIU Bao, WANG Xue-wen, MENG Yu-qi, WANG Xing-ming, WANG Ming-yu. Separation and recovery of Ni from copper electrolyte by crystallization of nickel ammonium sulfate double salt [J]. Transactions of Nonferrous Metals Society of China, 2022, 32(11): 3780−3789. https://doi.org/10.1016/S1003-6326(22)66057-6.

[6] DU Shou-ming, MU Wen-ning, LI Li-yin, SHI Shu-zheng, CHEN Huan-huan , LEI Xue-fei, GUO Rui, LUO Shao-hua, WANG Le. Simultaneous extraction of metals from nickel concentrate via NH_4HSO_4 roasting−water leaching process and transformation of mineral phase [J]. Transactions of Nonferrous Metals Society of China, 2024, 34(3): 1003−1015. https://doi.org/10.1016/S1003-6326(23)66449-0.

[7] SELVARAJ H, ARAVIND P, SUNDARAM M. Four compartment mono selective electrodialysis for separation of sodium formate from industry wastewater [J]. Chemical Engineering Journal, 2018, 333: 162−169. https://doi.org/10.1016/j.cej.2017.09.150.

[8] ÖZTÜRK Y, EKMEKÇI Z. Removal of sulfate ions from process water by ion exchange resins [J]. Minerals Engineering, 2020, 159: 106613. https://doi.org/10.1016/j.mineng.2020.106613.

[9] RANGE B M K, HAWBOLDT K A. Review: Removal of thiosalt/sulfate from mining effluents by adsorption and ion exchange [J]. Mineral Processing and Extractive Metallurgy Review, 2019, 40(2): 79−86. https://doi.org/10.1080/08827508.2018.1481062.

[10] TANG Bin, MU Ting-zhen, SHI Jian, YANG Mao-hua, XING Jian-min. A method and device for treating sulfur-containing wastewater: China, CN113880246A [P]. 2022−01−04. (in Chinese)

[11] LI Xue-long, MA Xiao-jun, WANG Shao-hua. The method of extracting ammonium thiocyanate and ammonium sulfate from ammonia desulfurization waste liquid of coke oven gas: China, CN108439430B [P]. 2020−08−25. (in Chinese)

[12] LU Yong-chao, GAO Qing-yu, XU Li, ZHAO Yue-min, EPSTEIN I R. Oxygen-sulfur species distribution and kinetic analysis in the hydrogen peroxide−thiosulfate system [J]. Inorganic Chemistry, 2010, 49(13): 6026−6034. https://doi.org/10.1021/ic100573a.

[13] FINDLAY A J, KAMYSHNY A. Turnover rates of intermediate sulfur species ($S_x^{(2-)}$), S^0, $S_2O_3^{2-}$, $S_4O_6^{2-}$, SO_3^{2-}) in anoxic freshwater and sediments [J]. Frontiers in Microbiology, 2017, 8: 292363. https://doi.org/10.3389/fmicb.2017.02551.

[14] GONZALEZ L J M, PATINO C F, ROCA V A, CRUELLS C M. Oxidation of thiosulfate with oxygen using copper (II) as a catalyst [J]. Metals, 2019, 9(4): 387. https://doi.org/10.3390/ met9040387.

[15] XU Hao-ran, WANG Tian, KOPPALA S, HU Jue, MA Shao-bin, MIAO Wen-long, LE T, ZHANG Li-bo. Improving the quality of ammonium sulfate produced from the flue gas desulfurization process by using ammonium persulfate [J]. Separation and Purification Technology, 2023, 308: 122879. https://doi.org/10.1016/ j.seppur.2022.122879.

[16] GB/T 535—2020. Fertilizer grade ammonium sulphate [S]. (in Chinese)

[17] DANEHY J P, ZUBRITSKY C W. Iodometric method for the determination of dithionite, bisulfite, and thiosulfate in the presence of each other and its use in following the decomposition of aqueous solutions of sodium dithionite [J]. Analytical Chemistry, 1974, 46(3): 391−395. https://doi.org/

10.1021/ac60339a022.

[18] DAUNORAVICIUS Z, PADARAUSKAS A. Capillary electrophoretic determination of thiosulfate, sulfide and sulfite using in-capillary derivatization with iodine [J]. Electrophoresis, 2002, 23(15): 2439−2444. https://doi.org/10.1002/1522-2683(200208)23: 15.

[19] YERMAKOV A N. Sulfite oxidation catalyzed by manganese (II) ions: Reaction kinetics in excess of metal ions [J]. Kinetics and Catalysis, 2021, 62(5): 565−572. https://doi.org/10.1134/s0023158421050013.

[20] WU Peng, JIN Xiao-jing, QIU Yong-cai, YE Dai-qi. Recent progress of thermocatalytic and photo/thermocatalytic oxidation for VOCs purification over manganese-based oxide catalysts [J]. Environmental Science & Technology, 2021, 55(8): 4268−4286. https://doi.org/10.1021/acs.est.0c08179.

[21] ROLIA E, CHAKRABARTI C L. Kinetics of decomposition of tetrathionate, trithionate, and thiosulfate in alkaline media [J]. Environmental Science & Technology, 1982, 16(12): 852−857. https://doi.org/10.1021/es00106a006.

[22] JAGUSHTE M V, MAHAJANI V V. Insight into spent caustic treatment: on wet oxidation of thiosulfate to sulfate [J]. Journal of Chemical Technology & Biotechnology, 1999, 74(5): 437−444. https://doi.org/10.1002/(SICI)1097-4660(199905)74:5<437::AID-JCTB63>3.0.CO; 2-1.

[23] LIAN Zheng, ZHU Chen-yu, ZHANG Shu-le, MA Wei-hua, ZHONG Qin. Study on the synergistic oxidation of sulfite solution by ozone and oxygen: Kinetics and mechanism [J]. Chemical Engineering Science, 2021, 242: 116745. https://doi.org/10.1016/j.ces.2021.116745.

[24] AHMAD N, AHMAD F, KHAN I, KHAN A D. Studies on the oxidative removal of sodium thiosulfate from aqueous solution [J]. Arabian Journal for Science and Engineering, 2015, 40(2): 289−293. https://doi.org/10.1007/s13369-014-1473-0.

[25] HUANG You-ju, LIN Yu-li, LI Wei-shan. Controllable syntheses of α- and σ-MnO_2 as cathode catalysts for zinc-air battery [J]. Electrochimica Acta, 2013, 99: 161−165. https://doi.org/10.1016/j.electacta.2013.03.088.

[26] QIN Qing-dong, WANG Qian-qian, FU Da-fang, MA Jun. An efficient approach for Pb(II) and Cd(II) removal using manganese dioxide formed in situ [J]. Chemical Engineering Journal, 2011, 172(1): 68−74. https://doi.org/10.1016/j.cej.2011.05.066.

[27] ANANTH M V, PETHKAR S, DAKSHINAMURTHI K. Distortion of MnO_6 octahedra and electrochemical activity of Nstutite-based MnO_2 polymorphs for alkaline electrolytes—An FTIR study [J]. Journal of Power Sources, 1998, 75(2): 278−282. https://doi.org/10.1016/S0378-7753(98)00100-1.

[28] SOCRATES G. Infrared and Raman characteristic group frequencies: Tables and charts [M]. New Jersey: John Wiley & Sons, 2004.

[29] ZELINSKII A G, NOVGORODTSEVA O N. The effect of solution pH on the oxidation of sulfite ions and the formation of oxides on the gold electrode [J]. Russian Journal of Electrochemistry, 2019, 55(12): 1171−1185. https://doi.org/10.1134/s1023193519120206.

[30] XIE Feng, CHEN Jun-nan, WANG Jian, WANG Wei. Review of gold leaching in thiosulfate-based solutions [J]. Transactions of Nonferrous Metals Society of China, 2021, 31(11): 3506−3529. https://doi.org/10.1016/S1003-6326(21)65745-X.

[31] ZHANG Hong-guang, DREISINGER D B. The kinetics for the decomposition of tetrathionate in alkaline solutions [J]. Hydrometallurgy, 2002, 66(1): 59−65. https://doi.org/10.1016/S0304-386X(02)00078-6.

[32] LI Wei, ZHOU Jing-hong, XIAO Wen-de. Oxidation of concentrated ammonium sulfite [J]. Journal of East China University of Science and Technology, 2001, 27(3): 226−229. (in Chinese). https://doi.org/10.14135/j.cnki.1006-3080.2001.03.002.

[33] KELEMEN S R, GEORGE G N, GORBATY M L. Direct determination and quantification of sulphur forms in heavy petroleum and coals: 1. The X-ray photoelectron spectroscopy (XPS) approach [J]. Fuel, 1990, 69(8): 939−944. https://doi.org/10.1016/0016-2361(90)90001-7

[34] KARIMI S, RASHCHI F, GHAHREMAN A. The evaluation of sphalerite surface formed during oxidative leaching in acidic ferric sulfate media [J]. Journal of Sustainable Metallurgy, 2021, 7(3): 1304−1313. https://doi.org/10.1007/s40831-021-00418-3.

[35] PENG Jian, YANG Zhen, LIAN Pei-chao. Kinetics of uncatalyzed oxidation of ammonium sulfite from wet ammonia desulfurization [J]. International Journal of Chemical Kinetics, 2023, 55(5): 238−246. https://doi.org/10.1002/kin.21631.

[36] HAN Rong, FANG Xi-hong, SONG Yun-hua, WANG Lei, LU Yuan, MA Hua-peng, XIAO Hao, SHAO Lei. Study on the oxidation of ammonium sulfite by ozone in a rotating packed bed [J]. Chemical Engineering and Processing: Process Intensification, 2022, 173: 108820. https://doi.org/10.1016/j.cep.2022.108820.

[37] HOLZ S, STEWERS L, THIELERT H, GUETTA Z, REPKE J U. Kinetic parameter identification and model discrimination using the example of the wet oxidation of thiosulfate [J]. Chemie Ingenieur Technik, 2020, 92(3): 209−220. https://doi.org/10.1002/cite.201900063. (in German)

[38] WURM J, PÖSCHMANN R, THIELERT H, von MORSTEIN O, REPKE J U. Kinetics of ammonium thiosulfate wet air oxidation under high-temperature conditions [J]. Chemical Engineering & Technology, 2022, 45(9): 1588−1597. https://doi.org/10.1002/ceat.202200098.

采用多级氧化方法高效氧化溶液中的硫代硫酸盐

徐浩然[1]，黄伟超[2]，A. V. RAVINDRA[3]，
Duc-lenh PHAN[4]，Thi-quynh-xuan LE[1]，张利波[1]，尹少华[1]

1. 昆明理工大学 冶金与能源工程学院，昆明 650093；
2. 中国稀土(广西)金源稀土新材料有限公司，贺州 542603；
3. Department of Physics and Nanotechnology, Faculty of Engineering and Technology,
SRM Institute of Science and Technology, Kattankulathur, Tamil Nadu, 603203, India;
4. Science and Technology Center, MienTrung Industry and Trade College, Phu Yen 56000, Viet Nam

摘　要：采用热力学计算和模拟脱硫溶液实验，分别研究亚硫酸盐和硫代硫酸盐在氧气和过硫酸盐氧化剂作用下氧化特性的差异。随后，提出一种新的氧气−过硫酸铵多级氧化方法，并将其应用于实际脱硫溶液的氧化。结果表明，实际脱硫溶液中硫代硫酸盐和亚硫酸盐的浓度分别从 48.76 和 61.76 g/L 降至 2.24 和 0.02 g/L，得到颗粒均匀的白色硫酸铵产品。此外，与单独使用过硫酸铵相比，多级氧化法可减少 37.56 %过硫酸铵添加量，降低处理成本 28.13%。

关键词：过硫酸铵；氧气；硫代硫酸盐；脱硫溶液；成本

(Edited by Xiang-qun LI)